Available online at www.sciencedirect.com

ScienceDirect

IFAC PapersOnline CONFERENCE PAPER ARCHIVE

IFAC PapersOnLine 51-22 (2018) 393–398

Humanoid Gait Generation on Uneven Ground using Intrinsically Stable MPC ⋆

Alessio Zamparelli Nicola Scianca Leonardo Lanari Giuseppe Oriolo

Dipartimento di Ingegneria Informatica, Automatica e Gestionale, Sapienza University of Rome, Italy
(e-mail: {scianca, lanari, oriolo}@diag.uniroma1.it)

Abstract: This paper presents a Model Predictive Control (MPC) scheme capable of generating a 3D gait for a humanoid robot. The proposed method starts from an assigned sequence of footsteps and generates online the trajectory of both the Zero Moment Point and Center of Mass. Starting from the moment balance (neglecting rotations) we derive a model characterizing all 3D trajectories that satisfy a linear differential equation along all three axes. Then a solution is found by extending our previously proposed intrinsically stable MPC, which employs a stability constraint for guaranteeing boundedness of the solution. The method is validated using a NAO robot in a simulated dynamic environment.

Keywords: Humanoid, Walking, Real-time, Predictive Control, Optimization

1. INTRODUCTION

Humanoid robots gained increasingly more attention in the last few years. However, the great advantage given by their versatility comes with multiple challenges that need to be solved in order to generate appropriate motions. When walking, the humanoid robot needs to maintain balance while regularly switching the contact with the ground. This is usually done by ensuring that the Zero Moment Point (ZMP) is at all times within the convex hull of the robot support polygon. Since this is a complex task, in order to generate such motions a simplified model which considers only the motion of the Center of Mass (CoM) is often employed. By neglecting the robot angular momentum the CoM dynamics can be treated as an Inverted Pendulum (IP). Moreover, assuming a flat ground and by constraining the CoM height to a constant value, the model becomes the Linear Inverted Pendulum (LIP) obtained by Kajita and Tani (1991). This allowed the derivation of control schemes for the generation of the CoM reference trajectory among which the Preview Control approach of Kajita et al. (2003) quickly became the most widespread. A notable improvement has been achieved by embedding Kajita's preview control approach in a Model Predictive Control (MPC) framework where hard constraints can be explicitly taken into account. This lead to the possibility of generating gaits with footsteps determined automatically (Herdt et al., 2010). With these assumptions the LIP is particularly suited for generating gaits on flat ground, since the constant height of the CoM can be simply enforced at the kinematic level.

On uneven terrain, however, we need to allow 3D CoM motions and thus the vertical displacement of the CoM which now behaves as a variable length IP. The corresponding model becomes nonlinear and the problem could be approached as in Caron and Kheddar (2017) where nonlinear constraints are introduced and a dual MPC scheme involving nonlinear optimization is used or, more recently, as in Caron et al. (2018) where capturability-based concepts are extended to the 3D case.

A simpler alternative considers pre-assigned vertical CoM motion and results in a time-varying IP frequency as in (Herdt, 2012; Hopkins et al., 2014). This idea was also used in (Kamioka et al., 2015) for the transition between bipedal and quadrupedal locomotion. The resulting system is linear time-varying and therefore the determination of suitable CoM motions remains still difficult in general.

It is however possible, while still allowing some vertical motion of the CoM, to remain in the LIP simple framework. A first important result is due to Terada and Kuniyoshi (2007) who constrain the motion of the CoM vertical component to satisfy a particular differential equation. The same idea has been developed in (Luo et al., 2013) introducing a 3D linear model which has a LIP-like dynamics also along the z-axis. A closely related approach has also been used in Englsberger et al. (2015).

Alternative ideas have been proposed in (Takenaka et al., 2009) studying the divergent component of motion for running which involves vertical acceleration of the center of gravity, in (Brasseur et al., 2015) using a linearized MPC to generate in real time walking motions over uneven terrain with guaranteed kinematic and dynamic feasibility, and in (Heerden, 2015) approaching the variable height CoM problem with a quadratically constrained quadratic program (QCQP) formulation and solving it via sequential quadratic programming (SQP).

Since the LIP has an unstable mode, one needs to ensure that the generated trajectories remain bounded. In a previous work (Scianca et al., 2016) we developed an MPC control scheme for gait generation that is guaranteed to produce bounded constant-height CoM trajectories by enforcing a stability constraint. In this paper we derive a

⋆ This work is supported by the EU H2020 project COMANOID.

10.1016/j.ifacol.2018.11.574

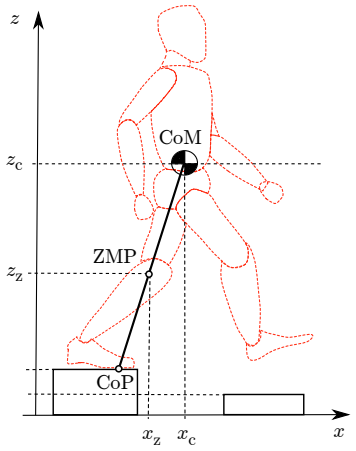

Fig. 1. A humanoid walking on piecewise-horizontal ground (side view). Note the relative positions of the CoM, the CoP and the ZMP.

linear model which allows vertical CoM motion and then design an intrinsically stable MPC for it, thus obtaining a gait generation method suitable for uneven ground.

The paper is organized as follows. Section 2 describes the proposed 3D motion model. The intriniscally stable MPC formulation and algorithm are presented in Sect. 3 and 4, respectively. Dynamic simulations of a gait on uneven ground are presented in Sect. 5. Section 6 offers some concluding remarks.

2. 3D MOTION MODEL

In this section we recall first the dynamic equations governing the 3D motion of the CoM for a humanoid walking on a specific kind of uneven ground. Then, we show how these dynamic equations become linear and time-invariant if the vertical motion of the CoM is appropriately constrained.

In the following we denote by (x_z, y_z, z_z) and (x_c, y_c, z_c) respectively the positions of the ZMP and of the CoM.

2.1 3D CoM dynamics

Throughout this paper, we will assume that the humanoid is walking on *piecewise-horizontal* ground, i.e., a composite surface made by horizontal patches located at different heights; for example, this is the case of a robot climbing or descending a staircase, or stepping over boxes of different sizes. In this situation, the gravity acceleration is always directed as the normal to the surface. Further, we will also suppose that the variation of the angular momentum around the CoM is negligible. These two assumptions lead to the situation shown in Fig. 1: at each step, the Center of Pressure (CoP) is located on the corresponding patch while the ZMP can be anywhere along the line joining the CoP and the CoM (Caron and Kheddar, 2017).

Under the above assumptions, moment balance around the ZMP for the x coordinate is expressed as

$$(z_c - z_z)\,\ddot{x}_c = (\ddot{z}_c + g)(x_c - x_z),$$

where g is the gravity acceleration. An identical balance equation can be written for the y coordinate. The two balance equations allow to write the dynamics of the x, y coordinates of the CoM as

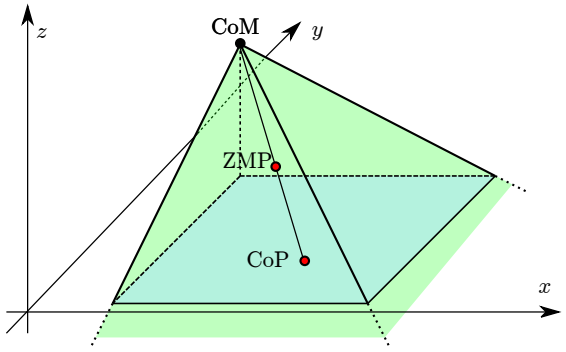

Fig. 2. Balance condition in 3D: the CoP should be internal to the support polygon (light blue). This is equivalent to requiring that the ZMP is internal to the polyhedral cone (green) with the CoM as vertex.

$$\ddot{x}_c = \frac{\ddot{z}_c + g}{z_c - z_z}(x_c - x_z) \tag{1}$$

$$\ddot{y}_c = \frac{\ddot{z}_c + g}{z_c - z_z}(y_c - y_z). \tag{2}$$

Force balance along the z axis leads to a structurally different dynamics for the corresponding coordinate:

$$\ddot{z}_c = \frac{f_z}{m} - g, \tag{3}$$

where f_z denotes the z-component of the ground reaction force, acting as an external input, and m is the total mass of the humanoid. For a detailed derivation of the above dynamic equations see, e.g., Kajita et al. (2014).

The condition for maintaining balance is that the CoP is internal to the support polygon, as this guarantees that the robot feet do not tilt w.r.t. the ground. Since the CoP, the CoM and the ZMP are colinear, the condition is equivalent to the ZMP being internal to the polyhedral cone having the CoM as vertex and the support polygon as cross-section, see Fig. 2.

2.2 3D Linear Model

The 3D motion model (1–3) is clearly nonlinear and therefore cumbersome to use for gait generation. The usual way to make the model linear is to assume that the ground is fully horizontal (i.e, all patches are at the same zero height) and that the CoM elevation over the ground is constant; as a consequence, we can set $z_z = 0$ (i.e., ZMP coincident with the CoP) and $z_c = \bar{z}_c$ constant, thus obtaining the well known LIP model

$$\ddot{x}_c = \omega_0^2\,(x_c - x_z)$$

$$\ddot{y}_c = \omega_0^2\,(y_c - y_z),$$

where $\omega_0^2 = g/\bar{z}_c$. This is a 2D linear model which is not appropriate for gait generation over uneven terrain.

However, requiring the CoM to move at a constant height is not the only way to make the system linear. A more general option is constraining its vertical motion so that

$$\frac{\ddot{z}_c + g}{z_c - z_z} = \omega^2, \tag{4}$$

with ω an arbitrary constant. The LIP model can then be seen as a particular case in which $\omega^2 = \omega_0^2$.

Using (4), eqs. (1–2) become

$$\ddot{x}_\mathrm{c} = \omega^2(x_\mathrm{c} - x_\mathrm{z}) \tag{5}$$

$$\ddot{y}_\mathrm{c} = \omega^2(y_\mathrm{c} - y_\mathrm{z}), \tag{6}$$

whereas the dynamics of z_c are directly derived from the constraint itself (4) as

$$\ddot{z}_\mathrm{c} = \omega^2\,(z_\mathrm{c} - z_\mathrm{z}) - g. \tag{7}$$

The dynamic equations (5–7) are linear (strictly speaking, affine) and have a clear LIP-like structure, with the ZMP coordinates (x_z, y_z, z_z) acting as control inputs. This 3D model allows vertical motion of the CoM and therefore can be used for gait generation on uneven terrain, in conjunction with the balance condition illustrated in Fig. 2.

Note the following points.

- Comparing the constrained dynamics (7) of z_c with its free dynamics (3), we can derive the required vertical component of the ground reaction force as
$$f_z = m\,\omega^2\,(z_\mathrm{c} - z_\mathrm{z}),$$
i.e., a force proportional to the vertical displacement between the CoM and the ZMP.
- The value of ω determines the equilibrium point of the z_c dynamics, which is met when the difference between the z coordinates of the ZMP and CoM is equal to g/ω^2; i.e., when the reaction force f_z equals the gravitational force. Being a design parameter of our approach, ω can be freely chosen as long as it is compatible with the robot kinematic limits.

3. MPC FORMULATION

Under the assumption that the footstep sequence is assigned in advance, we now describe an MPC scheme for gait generation that is based on the 3D model (5–7). It is important to note that all three equations include an unstable subsystem, which will be taken care of by adding a stability constraint. The proposed method represents an extension to the 3D case of the result in Scianca et al. (2016).

3.1 Motion model

To improve the smoothness of the generated trajectories we perform a dynamic extension and choose the control variable as the ZMP velocity $\dot{x}_\mathrm{z}$ rather than the ZMP itself. On the x axis we have then

$$\begin{pmatrix} \dot{x}_\mathrm{c} \\ \ddot{x}_\mathrm{c} \\ \dot{x}_\mathrm{z} \end{pmatrix} = \begin{pmatrix} 0 & 1 & 0 \\ \omega^2 & 0 & -\omega^2 \\ 0 & 0 & 0 \end{pmatrix} \begin{pmatrix} x_\mathrm{c} \\ \dot{x}_\mathrm{c} \\ x_\mathrm{z} \end{pmatrix} + \begin{pmatrix} 0 \\ 0 \\ 1 \end{pmatrix} \dot{x}_\mathrm{z}. \tag{8}$$

The dynamics are the same along all three axes, with the exception of the additive term g appearing in the second equation of the dynamics along the z axis, see (7).

We will use piecewise-constant control inputs over sampling intervals of duration δ, with a prediction horizon $T_\mathrm{h} = N \cdot \delta$. We denote the current time instant by t_k and the successive instants within the prediction horizon by t_{k+i}, $i = 1, \ldots, N$. A similar notation is used for all variables; e.g., the current CoM position is x_c^k and its predicted value at t_{k+i} is x_c^{k+i}. At a generic instant t_j we have

$$\dot{x}_\mathrm{z}(t) = \dot{x}_\mathrm{z}^j, \quad t \in [t_j, t_{j+1}),$$

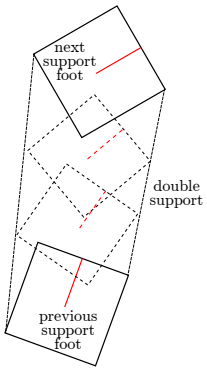

Fig. 3. The moving ZMP constraint (dashed region) during double support.

so that the ZMP x-position in the time interval $[t_j, t_{j+1}]$ is

$$x_\mathrm{z}(t) = x_\mathrm{z}^j + (t - t_j)\,\dot{x}_\mathrm{z}^j, \quad t \in [t_j, t_{j+1}]. \tag{9}$$

3.2 ZMP constraints

We briefly recall how the ZMP constraints can be imposed in the 2D case (Scianca et al., 2016), and then discuss how this can be done in the 3D case.

Recall that when walking on fully horizontal ground the robot maintains balance if the ZMP remains inside the support polygon. Denote by $(x_\mathrm{f}^j, y_\mathrm{f}^j)$ and θ_f^j respectively the position and orientation of the generic footstep within the assigned sequence. We use a fixed-shape *moving* ZMP constraint to enforce balance: in particular, the admissible region for the ZMP at t_{k+i} is centered in $(x_\mathrm{f}^{k+i}, y_\mathrm{f}^{k+i})$ and has orientation θ_f^{k+i}, with these values defined as follows:

- in single support, $(x_\mathrm{f}^{k+i}, y_\mathrm{f}^{k+i})$ and θ_f^{k+i} coincide with the position and orientation of the support foot, respectively $(x_\mathrm{f}^j, y_\mathrm{f}^j)$ and θ_f^j;
- in double support, $(x_\mathrm{f}^{k+i}, y_\mathrm{f}^{k+i})$ and θ_f^{k+i} gradually slide from the position and orientation of the previous support foot to those of the next (see Fig. 3).

This is a convenient way to enforce a double support constraint because, although not strictly necessary when the footsteps sequence is assigned, it generalizes easily to the case of automatically placed footsteps as described in (Aboudonia et al., 2017).

The expression of the ZMP constraint in 2D can then be written as

$$-\frac{1}{2}\begin{pmatrix} d_x^\mathrm{z} \\ d_y^\mathrm{z} \end{pmatrix} \leq R_{k+i}^T \begin{pmatrix} x_\mathrm{z}^{k+i} - x_\mathrm{f}^{k+i} \\ y_\mathrm{z}^{k+i} - y_\mathrm{f}^{k+i} \end{pmatrix} \leq \frac{1}{2}\begin{pmatrix} d_x^\mathrm{z} \\ d_y^\mathrm{z} \end{pmatrix}, \tag{10}$$

where d_x^z and d_y^z are the dimensions of the rectangular constraint region and R_{k+i}^T is the rotation matrix associated with θ_f^{k+i}. Note that $(x_\mathrm{z}^{k+i}, y_\mathrm{z}^{k+i})$ is the predicted position of the ZMP, which can be expressed as a linear combination of the control variables using (9); e.g., for the x coordinate we get

$$x_\mathrm{z}^{k+i} = x_\mathrm{z}^k + \delta \sum_{j=0}^{i-1} \dot{x}_\mathrm{z}^{k+j}. \tag{11}$$

Constraint (10) must be imposed for $i = 1, \ldots N$, leading to a total of N constraints.

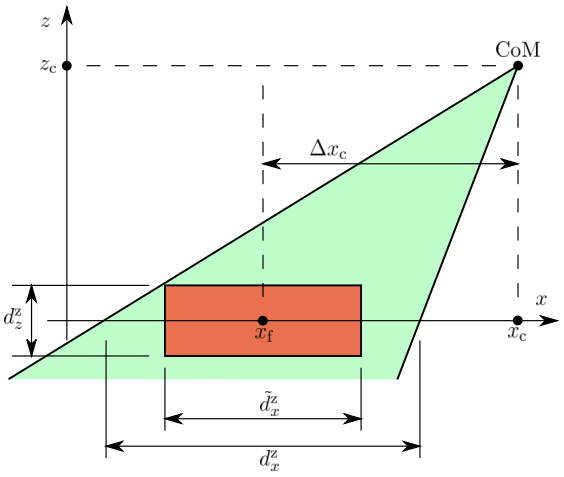

Fig. 4. Side view of the polyhedral cone (green) representing the actual ZMP constraint and the box (red) used for defining approximate linear constraint. Here, the CoM is at its maximum allowed displacement Δx_c with respect to the center of the support foot.

In the 3D case, the ZMP is allowed to leave the ground in order to generate vertical CoM motions, and correspondingly $\dot{z}_z^{k+i}$ has become a control variable. As illustrated in Fig. 2, the balance condition now requires the ZMP to remain inside the polyhedral cone defined by the support polygon and the CoM. However, when the ZMP is allowed to move vertically the cone defines a nonlinear constraint. In order to remove this nonlinearity, a box constraint is used instead (see Fig. 4):

$$-\frac{1}{2}\begin{pmatrix}\tilde{d}_x^z\\ \tilde{d}_y^z\\ d_z^z\end{pmatrix} \leq R_{k+i}^T \begin{pmatrix}x_z^{k+i}-x_f^{k+i}\\ y_z^{k+i}-y_f^{k+i}\\ z_z^{k+i}-z_f^{k+i}\end{pmatrix} \leq \frac{1}{2}\begin{pmatrix}\tilde{d}_x^z\\ \tilde{d}_y^z\\ d_z^z\end{pmatrix}, \quad (12)$$

where d_z^z is a design parameter that defines the maximum allowed vertical ZMP displacement w.r.t. the horizontal patch. To guarantee that the box is contained in the cone, its x and y dimensions are reduced to $\tilde{d}_x^z$ and $\tilde{d}_y^z$. Suitable values for these parameters are

$$\tilde{d}_x^z = d_x^z\left(1-\frac{d_z^z}{2z_c^{\min}}\right) - \frac{d_z^z}{z_c^{\min}}\Delta x_c,$$

where Δx_c is the maximum expected displacement of the CoM with respect to the center of the support foot and $z_c^{\min}$ is the minimum expected value for the CoM height. An analogous formula can be written for $\tilde{d}_y^z$.

Similarly to the 2D case, the box constraint is kept fixed during single support. During double support, the box slides linearly from its position around the previous support foot to its position around the next support foot, thus always remaining within the polyhedral cone which defines the ZMP balance constraint for this situation (see Fig. 5).

3.3 Stability constraint

As already mentioned, the motion model (5–7) is unstable and thus its generic solution diverges, making all components of the CoM position unbounded w.r.t. the ZMP position and the generated gait ultimately unfeasible.

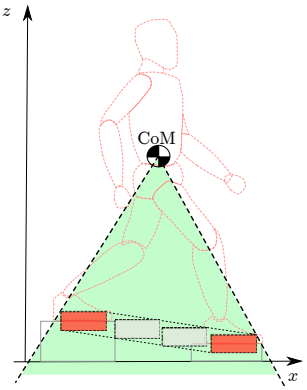

Fig. 5. During double support, the box constraint slides from the previous to the next support foot.

In (Scianca et al., 2016) it was shown that if the initial condition $(x_c^k, \dot{x}_c^k)$ satisfies

$$x_c^k + \frac{\dot{x}_c^k}{\omega} = \omega\int_{t_k}^{\infty} e^{-\omega(\tau-t_k)}x_z(\tau)d\tau, \quad (13)$$

then the solution of (5) remains bounded w.r.t. x_z for all t. A similar condition can be written for the y_c dynamics (6) while for z_c we obtain a slightly different condition

$$z_c^k + \frac{\dot{z}_c^k}{\omega} = \frac{g}{\omega^2} + \omega\int_{t_k}^{\infty} e^{-\omega(\tau-t_k)}z_z(\tau)d\tau. \quad (14)$$

In the MPC formulation, the stability condition (13) can be enforced by writing it as a constraint on the control variables $\dot{x}_z^{k+i}$:

$$\frac{1}{\omega}\frac{1-e^{-\delta\omega}}{1-e^{-N\delta\omega}}\sum_{i=0}^{N-1} e^{-i\delta\omega}\dot{x}_z^{k+i} = x_c^k + \frac{\dot{x}_c^k}{\omega} - x_z^k. \quad (15)$$

This expression is actually obtained by computing the integral in (13) using the piecewise linear ZMP trajectory (9), which however only goes up to the prediction horizon. The contribution beyond the horizon is computed by assuming *infinite replication* of the control variables [1] within T_h, the rationale being that the generated gait is expected to be cyclic and therefore exhibit some form of periodicity. An identical constraint can be written for the y_c component.

The stability constraint on the z_c component is derived from (14) as

$$\frac{1-e^{-\delta\omega}}{\omega}\sum_{i=0}^{N-1} e^{-i\delta\omega}\dot{z}_z^{k+i} = z_c^k + \frac{\dot{z}_c^k}{\omega} - z_z^k - \frac{g}{\omega^2}. \quad (16)$$

This expression is not based on an infinite replication assumption since on uneven terrain vertical motions cannot be expected to be cyclic. Rather, $\dot{z}_z$ is simply set to zero beyond the prediction horizon.

4. MPC ALGORITHM

Having defined the constraints, we now briefly illustrate the MPC algorithm which solves a Quadratic Programming (QP) problem at each iteration. We assume that the coordinates of the footsteps are assigned. To extend the proposed algorithm to the case of automatic footsteps

[1] To this end, it is assumed that the prediction horizon T_h is a multiple of the step duration.

placement in the x and y directions with known footsteps height z_{f}^j, a Mixed-Integer quadratic programming approach can be used.

4.1 Formulation of the QP problem

Defining the decision variables vectors

$$\dot{X}_{\mathrm{z}}^k = (\dot{x}_{\mathrm{z}}^k \ \ \dots \ \ \dot{x}_{\mathrm{z}}^{k+N-1})^T$$
$$\dot{Y}_{\mathrm{z}}^k = (\dot{y}_{\mathrm{z}}^k \ \ \dots \ \ \dot{y}_{\mathrm{z}}^{k+N-1})^T$$
$$\dot{Z}_{\mathrm{z}}^k = (\dot{z}_{\mathrm{z}}^k \ \ \dots \ \ \dot{z}_{\mathrm{z}}^{k+N-1})^T,$$

the QP problem is written as

$$\min_{\dot{X}_{\mathrm{z}}^k, \dot{Y}_{\mathrm{z}}^k, \dot{Z}_{\mathrm{z}}^k} \sum_{i=1}^{N} \left((\dot{x}_{\mathrm{z}}^{k+i})^2 + (\dot{y}_{\mathrm{z}}^{k+i})^2 + (\dot{z}_{\mathrm{z}}^{k+i})^2 + \beta (z_{\mathrm{z}}^{k+i} - z_{\mathrm{f}}^{k+i})^2 \right)$$

subject to:
ZMP constraints (12)
stability constraints for x, y and z (15) and (16)

where the cost function includes the decision variables for regularization purposes and a term which attempts to bring the ZMP to patch level whenever possible.

4.2 Algorithm

We now provide a sketch of the MPC algorithm. The position of each assigned footstep, together with its timing, is used to compute the box constraint for the ZMP using the moving constraint procedure described in Sect. 3.2. The MPC iteration starts at t_k and goes as follows.

(1) Compute $\dot{X}_{\mathrm{z}}^k, \dot{Y}_{\mathrm{z}}^k, \dot{Z}_{\mathrm{z}}^k$ that solve the QP problem.
(2) From the solutions, extract the first control samples $\dot{x}_{\mathrm{z}}^k$, $\dot{y}_{\mathrm{z}}^k$, $\dot{z}_{\mathrm{z}}^k$.
(3) Set $\dot{x}_{\mathrm{z}} = \dot{x}_{\mathrm{z}}^k$ in (8) and integrate from $(x_{\mathrm{c}}^k, \dot{x}_{\mathrm{c}}^k, x_{\mathrm{z}}^k)$ to obtain $x_{\mathrm{c}}(t)$, $\dot{x}_{\mathrm{c}}(t)$, $\dot{x}_{\mathrm{z}}(t)$ for $t \in [t_k, t_{k+1}]$. Similarly for the y and z components. This defines the 3D trajectory of the CoM during the considered time interval.

5. SIMULATIONS

We performed both MATLAB and dynamic simulations to illustrate the proposed approach. Commands for the robot joints are computed by a simple kinematic control law based on pure pseudoinversion that tracks the CoM trajectory produced by the MPC scheme, in addition to the swing foot trajectory, which is exogenous.

Figure 6 shows the results of a gait generation performed in MATLAB using the presented 3D model. The footsteps sequence is assigned so as to follow the profile of a small staircase, with two ascending steps followed by two descending ones. The ZMP trajectory along the z axis tries to pass through the footsteps while simultaneously driving the CoM trajectory to satisfy (7). In this simulation we chose the constant parameter $\omega = 6.14\ \mathrm{s}^{-1}$, duration of the single and double support respectively 0.2 s and 0.1 s, prediction time 0.6 s, the size of the constraints $d_x^{\mathrm{z}} = d_y^{\mathrm{z}} = 0.06$ m and $d_z^{\mathrm{z}} = 0.02$ m, while the maximum horizontal deviation of the CoM w.r.t. the footstep position is $\Delta x_{\mathrm{c}} = 0.15$ m. The sampling time is $\delta = 0.05$ s.

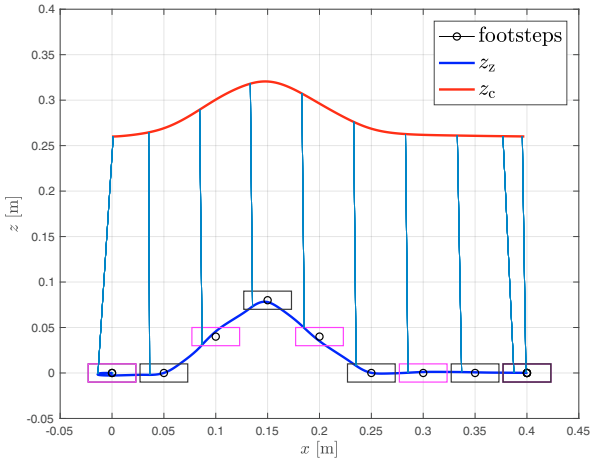

Fig. 6. MATLAB simulation: staircase example. The vertical lines represent the ZMP-CoM segment (i.e., the LIP) at the beginning of every single support.

We performed two dynamic simulations to show how this control scheme can effectively be employed on a humanoid robot walking while maintaining balance. The dynamic environment used is DART (Dynamic Animation and Robotics Toolkit), while qpOASES is used to solve the QP problem.

The first experiment requires the humanoid to step on boxes with variable height. A series of snapshots are shown in Fig. 7 which illustrate how the robot is able to keep balance while properly adapting the CoM trajectory, along the vertical direction, to the profile of the ground.

Snapshots from the second experiment are shown in Fig. 8. Here the algorithm is used to achieve a different task than walking on uneven terrain. The robot is required to walk on a flat ground while lowering its CoM for a few steps, after which it should come back to the initial height. This could be useful for avoiding obstacles hanging from the ceiling or to pick up items from the ground. If the final height is different from the initial one, it could also represent the transition from a biped to a quadruped locomotion as in (Kamioka et al., 2015). We achieve this behavior by lowering the center of the ZMP constraint (the red box in Fig. 4) below the ground, which is acceptable up to a certain extent because it is still contained within the conic region. Since the center of this constraint was taken to be coincident with the position of the center of the footstep, we temporarily set the footstep to be at ground level in order for the robot to not push into the ground while stepping.

Both dynamic simulations use the following parameters: $\omega = 6.14\ \mathrm{s}^{-1}$, single support and double support duration respectively 0.3 s and 0.2 s, prediction time 1.0 s, the size of the constraints $d_x^{\mathrm{z}} = d_y^{\mathrm{z}} = 0.03$ m and $d_z^{\mathrm{z}} = 0.02$ m, $\Delta x_{\mathrm{c}} = 0.15$ m, sampling time $\delta = 0.05$ s.

6. CONCLUSIONS

We presented an MPC for generating 3D CoM trajectories suitable for walking on uneven grounds. The CoM dynamics are rendered linear while still allowing vertical motions

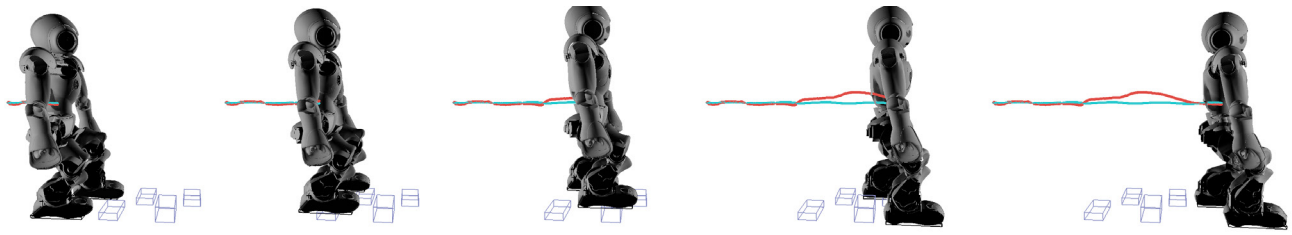

Fig. 7. Dynamic simulation: NAO stepping on small boxes with variable height. In red the trajectory of the CoM, in blue the same trajectory without the vertical variation.

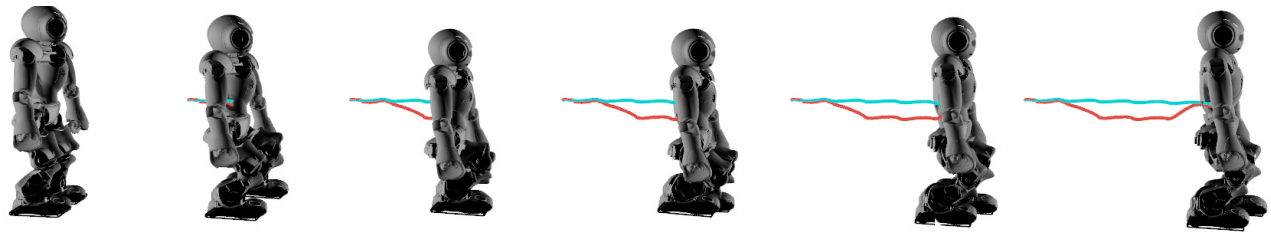

Fig. 8. Dynamic simulation: NAO lowering its center of mass while walking on a flat horizontal floor. In red the trajectory of the CoM, in blue the same trajectory without the vertical variation.

of the CoM, thus favoring the use of real-time optimization techniques. We illustrated the proposed approach on a NAO humanoid in a simulated dynamic environment. An experimental validation is under way. In the future, we will address the automatic footstep placement problem and study walking on inclined surfaces as well as in the presence of obstacles (De Simone et al., 2017).

REFERENCES

Aboudonia, A., Scianca, N., De Simone, D., Lanari, L., and Oriolo, G. (2017). Humanoid gait generation for walk-to locomotion using single-stage MPC. In *17th IEEE-RAS Int. Conf. on Humanoid Robots*, 178–183.

Brasseur, C., Sherikov, A., Collette, C., Dimitrov, D., and Wieber, P.B. (2015). A robust linear mpc approach to online generation of 3d biped walking motion. In *15th IEEE-RAS Int. Conf. on Humanoid Robots*, 595–601.

Caron, S. and Kheddar, A. (2017). Dynamic walking over rough terrains by nonlinear predictive control of the floating-base inverted pendulum. In *2017 IEEE/RSJ Int. Conf. on Intelligent Robots and Systems*, 5017–5024.

Caron, S., Escande, A., Lanari, L., and Mallein, B. (2018). Capturability-based analysis, optimization and control of 3d bipedal walking. *arXiv:1801.07022*.

De Simone, D., Scianca, N., Ferrari, P., Lanari, L., and Oriolo, G. (2017). MPC-based humanoid pursuit-evasion in the presence of obstacles. In *2017 IEEE/RSJ Int. Conf. on Intelligent Robots and Systems*.

Englsberger, J., Ott, C., and Albu-Schäffer, A. (2015). Three-dimensional bipedal walking control based on divergent component of motion. *IEEE Transactions on Robotics*, 31(2), 355–368.

Heerden, K.V. (2015). Planning com trajectory with variable height and foot position with reactive stepping for humanoid robots. In *2015 IEEE Int. Conf. on Robotics and Automation*, 6275–6280.

Herdt, A. (2012). *Model predictive control of a humanoid robot*. Ph.D. thesis, Ecole Nationale Supérieure des Mines de Paris.

Herdt, A., Diedam, H., Wieber, P.B., Dimitrov, D., Mombaur, K., and Diehl, M. (2010). Online walking motion generation with automatic footstep placement. *Advanced Robotics*, 24(5-6), 719–737.

Hopkins, M.A., Hong, D.W., and Leonessa, A. (2014). Humanoid locomotion on uneven terrain using the time-varying divergent component of motion. In *14th IEEE-RAS Int. Conf. on Humanoid Robots*, 266–272.

Kajita, S., Kanehiro, F., Kaneko, K., Fujiwara, K., Harada, K., Yokoi, K., and Hirukawa, H. (2003). Biped walking pattern generation by using preview control of zero-moment point. In *2003 IEEE Int. Conf. on Robotics and Automation*, 1620–1626.

Kajita, S. and Tani, K. (1991). Study of dynamic biped locomotion on rugged terrain-derivation and application of the linear inverted pendulum mode. In *1991 IEEE Int. Conf. on Robotics and Automation*, 1405–1411.

Kajita, S., Hirukawa, H., Harada, K., and Yokoi, K. (2014). *Introduction to Humanoid Robotics*. Springer.

Kamioka, T., Watabe, T., Kanazawa, M., Kaneko, H., and Yoshike, T. (2015). Dynamic gait transition between bipedal and quadrupedal locomotion. In *2015 IEEE/RSJ Int. Conf. on Intelligent Robots and Systems*, 2195–2201.

Luo, S.C., Chang, P.H., Sheng, J., Gu, S.C., and Chen, C.H. (2013). Arbitrary biped robot foot gaiting based on variate com height. In *13th IEEE-RAS Int. Conf. on Humanoid Robots*, 534–539.

Scianca, N., Cognetti, M., De Simone, D., Lanari, L., and Oriolo, G. (2016). Intrinsically stable MPC for humanoid gait generation. In *16th IEEE-RAS Int. Conf. on Humanoid Robots*, 601–606.

Takenaka, T., Matsumoto, T., Yoshiike, T., and Shirokura, S. (2009). Real time motion generation and control for biped robot - 2nd report: running gait pattern generation. In *2009 IEEE/RSJ Int. Conf. on Intelligent Robots and Systems*, 1092–1099.

Terada, K. and Kuniyoshi, Y. (2007). Online gait planning with dynamical 3d-symmetrization method. In *7th IEEE-RAS Int. Conf. on Humanoid Robots*, 222–227.